Implementation and Performance Assessment of Fast Active Power Injection Method for Type 4 Wind Turbine based on Real-time Simulation

Elyas Rakhshani [(1)], Nidarshan Veerakumar [(1)], Zameer Ahmad [(1)], José Rueda Torres [(1)], Mart A.M.M. van der Meijden [(1), (2)] and Peter Palensky [(1)]

[(1)] Department of Electrical Sustainable Energy, Delft University of Technology (TUD), Netherlands

[(2)] TenneT TSO B.V, Arnhem, Netherlands

***Abstract*— This paper deals with the implementation of a Fast Active Power Injection (FAPI) controller in a Type-4 Wind Turbine. Two different FAPI controllers, droop-based and a modified derivative-based controller are proposed and investigated under real-time simulation platform. The implementation is done in a Real-Time Digital Simulator (RTDS) by using the functionalities of RSCAD software. The IEEE 9 bus system is taken as a case study to quantitatively check the suitability of the implemented controller. The response of the wind turbine observed in EMT simulations is compared against the response obtained via numerical simulations with a generic wind turbine model built-in DIgSILENT PowerFactory software. The details of the model implemented in RSCAD provides better insight on capturing the impacts of controller parameters. Obtained results clearly demonstrate how the proposed controller can effectively improve the dynamic frequency performance of the power system.**

Keywords—Fast active power injection, Inertia emulation, Frequency control, MIGRATE, Type-4 Wind Turbine, RTDS, PowerFactory.

I. INTRODUCTION

Frequency stability is the ability of a power system to maintain steady-state frequency, following a severe system disturbance, resulting in a significant imbalance between generation and load [1]-[4]. It depends on the ability to restore the equilibrium between system generation and load demand with minimum loss of loads. This ability can be especially limited in modern power systems with low inertia [5]-[8]. Systems with low inertia are the result of the phase-out of the conventional power plants, with a synchronous generator, due to increasing the share of power electronic interfaced generation (PEIG) like solar photovoltaic systems and wind power plants [9]-[13]. Considering the intermitted behaviour in this kind of system, developing an additional supplementary control loop for facilitating fast frequency response (FFR) or Fast Active Power Injection (FAPI) capabilities of power electronics-based generation units are very important.

FAPI is essentially a mechanism to quickly regulate the active power injection to mitigate frequency variations in low inertia systems. Since it may overlap with the time window of the inertial response of conventional synchronous generators (0.5 s from the occurrence of an active power imbalance), some authors use the alternative term 'inertia emulation' (IE) [14]-[15]. The actual source of energy for emulating inertia in this study is the mechanical part of the wind turbine. A supplementary control loop for inertia emulation (IE) enables the wind turbine, to release the stored kinetic energy within 10s to arrest the frequency deviation that occurs after the occurrence of an imbalance of active power [12]-[13].

Existing literature shows that inertia emulation control can be implemented in different ways, ranging from de-loading technique [15], inertial based control [16]-[18], to proportional (droop) based controls [19]-[22]. It is worth mentioning that, in droop based approach it mainly contribute on improving the Nadir value, while the application of inertial based control alone, due to its limitation with noise amplification, might also be complicated. Therefore, a combination of different methods like proportional (droop) and derivative controls can be considered as an attractive option for enabling FAPI capabilities of the wind generation unit.

In this paper, a derivative based FAPI controller for enhancing the dynamic performance of system frequency is proposed and compared with the droop based controller for further analysis in different simulation platforms. The proposed method is a combination of both droop and derivative controls. The addition of droop based control is considered as a complementary control action to produce a change in the power reference, extracted from wind power, in proportion to the system frequency deviation for better recovery and enhancement of Nadir. The main goal of this paper is to implement and analyse a suitable FAPI controller for the wind turbine Type-4 in different simulation platforms (RMS and EMT). A plausible generic test bench was built in both PowerFactory (RMS) and RSCAD (EMT). FAPI controllers were implemented in both the platforms and it was made sure that initial conditions of both models were similar. Thus, in addition to the implementation of the FAPI controller in RSCAD platform, a complete set of sensitivity analysis to identify the impacts of different controller gains on system performance is presented. Here the limitations on details of the model components, like simplification of DC-link or averaged based models like in RMS is eliminated. Thus EMT based simulation models in RSCAD are performed to provide better insight on capturing the complete dynamic behaviour of the network under high generation-load imbalance conditions [23]-[24]. The EMT (Electro-magnetic Transient) studies in this paper were performed in RSCAD software package which runs on Real-Time Digital Simulator (RTDS). The models considered here are of full-scale, which means it includes all the controls and power system components present in an actual real system. By this, it can be ensured that the behaviour of all FAPI controllers along with their performance limitations is considered.

The rest of the paper is structured as the following. In Section II, the fast active power injection approach and the wind turbine control structure is presented. Later, in Section III, the studied case study used for performing comparisons and evaluations between RMS and EMT simulation for different FAPI controllers are described and discussed. And, finally, the paper is concluded in Section IV.

II. FAPI Controller for Wind Generation

In this study, the FAPI controller is implemented for a generic model of type 4 wind turbine. The general control structure of the wind turbine is developed based on IEC 61400-27 standard model [22]. Additional controllers were added as shown in Fig. 1 to consider IE and modified P and Q control channels. FAPI controllers are implemented inside of IE controller block shown in Figure 1.

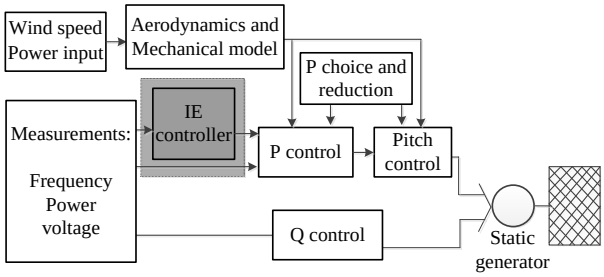

Figure 1. Controllers considered in the model of type 4 wind turbine.

A. *Droop-based fast active power controller*

The general structure of the droop based fast active power controller is presented in Fig. 2. The controller is the added IE controller block, which implies that the wind generator can react to a drop in system frequency (50Hz/60Hz) by temporarily increasing the wind turbine active power output. The energy for this increase is drawn from the rotating masses of the wind turbine. The mechanism of droop based FAPI controller is according to its output which will generate an additional reference signal for the output power of the wind turbine. This output signal, called delta_P_emu_ref, can be selected by proper tuning of controller gain K. Recalling Figure 2, the value of K can be tuned in such a way that there is linear dependency with respect to the total power output extracted from the wind generators due to droop based FAPI controller.

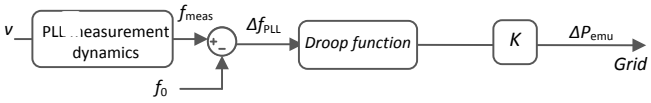

Figure 2. Block diagram of droop based FAPI controller.

B. *Derivative-based fast active power controller*

Derivative-based control approach for frequency mitigation is a strategy where the active power is injected/extracted based on the derivative of frequency from nominal frequency (50Hz / 60Hz) under the condition of dynamically changing loads/generations. Figure 3, illustrates the combined proposed derivative-based FAPI controller for the wind generator. In this controller, as the name suggests there are two controllers, namely droop controller and derivative controller.

As shown in Figure 3, in addition to the action of the droop term, the derivative term will have an additional impact, during containment period after the occurrence of the fault, on improving the slope of frequency response. This control loop takes the frequency error as input, which can pass through a combination of a low-pass filter and a derivative term. Thus, for any varying error signal (as the input of this controller), the combined low pass and derivative block reflect a value which is the derivative or slope of the input error signal (basically higher the frequency change, larger is the RoCoF value). The parameters for the low pass and the derivative control gain (Kd) are selected accordingly to achieve a proper response at the output of the controller.

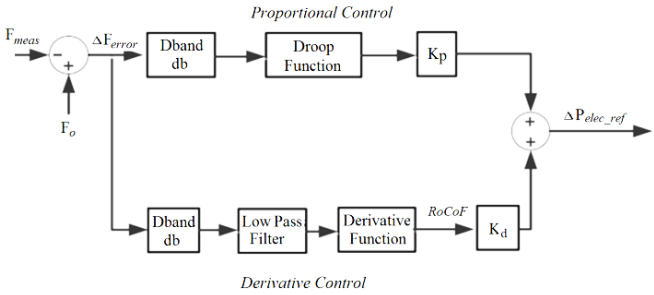

Figure 3. Combined block diagram of droop and derivative-based FAPI

Figure 4, is also presenting the outer loop controller of a wind generator which is responsible for generating the reference current from the electrical active power output of the wind generator (PM). As shown in Figures 4, the output signal of FAPI controller is added as an additional reference signal (named as del_P_{emu_ref} in RSCAD) to the electrical power reference signal on the Rotor Side Converter (RSC) which is responsible for setting the electrical power demand required from the permanent magnet synchronous machine (PMSM). So, with an additional reference from the droop controller, the electrical power reference could be altered. Accordingly, it would be possible to increase actual electrical power output from the Wind generators by setting a higher value for this additional reference signal from FAPI, but since the wind speed is kept constant and no changes are made in the pitch angle controller, mechanical power governed by wind speed is unaltered. This difference in electrical power and mechanical power will result in a decrease in speed and increase in torque at the wind turbine. Thus, depicting the extraction of kinetic energy from the wind turbine to emulate inertia. Also, it is observed that, bigger the wind turbines, higher will be the power rating, larger will be the inertia constant H of wind turbine and thus more power extraction is possible.

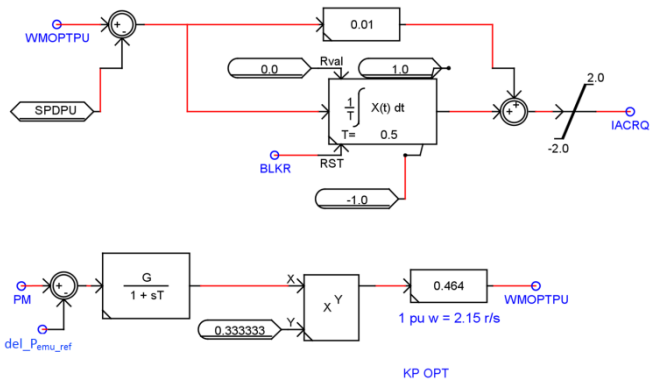

Figure 4. Snapshot of the outer loop controller implemented in RSCAD.

This issue and the impact of FAPI controller tunings on wind turbine behaviours are explained in more details in Section IV.

III. Test Case Results and Discussions

In this section, a plausible generic test system is developed as shown in Figure 5. This test bench consists of two synchronous generators and two wind turbines constituting a 52% wind share. Table 1 describes the load flow results with test case working stable under normal operation.

Table 1. Load flow results from a test system with 52% wind share.

Load Flow Results		P (MW)	Q (MVAR)
Generations	G1	73.4	33.8
	WG1	82.6	0
	G1	78.2	-1.8
	WG2	84	0
Loads	L5	125	50
	L6	90	30
	L8	100	35

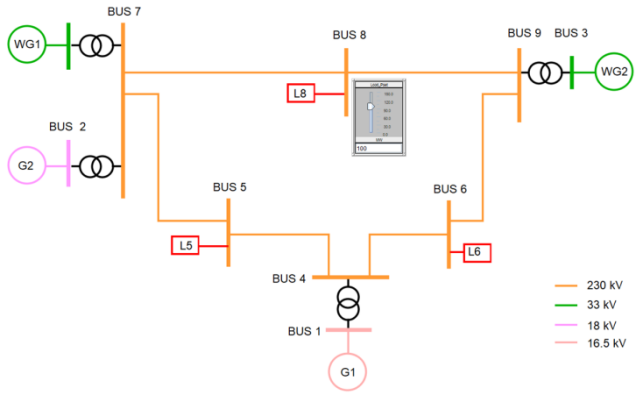

Figure. 5. IEEE 9 bus system with a 52% share of wind generation.

In this scenario, bus 8 was selected to create an under-frequency event (load increase) because the disturbance caused at this bus had the highest impact on Bus 2 and Bus 3, where the wind turbines are connected. Thus, to create an under-frequency event the load at bus 8 had to be suddenly increased. From literature, it was found that any sudden load frequency variation of 3% to 5% was considered as a major under-frequency event [25]. Figures 6 and 7 depict the response of frequency and power in pu delivered by synchronous generators and wind generators for 3% to 5% increase in load.

It can be observed that under normal operation without FAPI controllers active, the wind generators do not participate in the load frequency variation due to the presence of an AC-DC-AC full converter. Also, with higher imbalance, larger frequency deviation was observed. Please note that for all further analysis, a load disturbance of 5% shall be applied and frequency measurement which is required as an input to the FAPI controllers is measured at bus 8.

Therefore, the load at bus 8 had a step-wise sudden increase of around 5% at 2 s. Figure 8 represents the frequency plots extracted from EMT (RSCAD) and RMS (PowerFactory) models for a 5% load increase event at bus 8. Both graphs show similar frequency trends, but EMT plot depicts a higher slope of frequency before Nadir compared to RMS plot, which is due to the fact that the model built in EMT model is more vulnerable to load frequency disturbance compared to RMS.

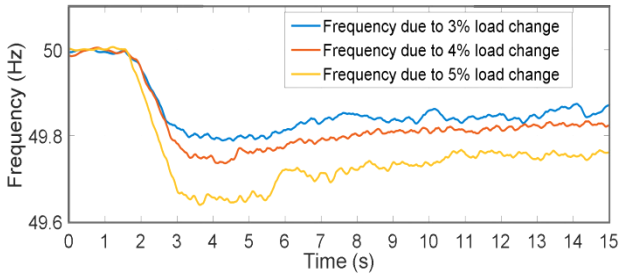

Figure 6. Frequency response due to load increase at bus 8.

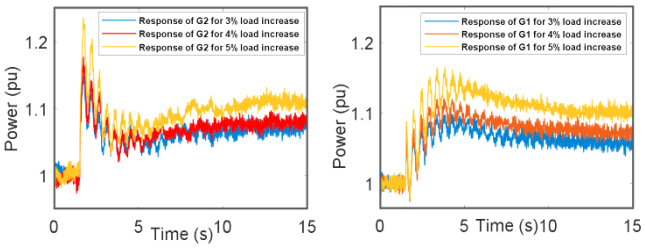

Figure 7. Power response at various generator terminals due to load increase at bus 8.

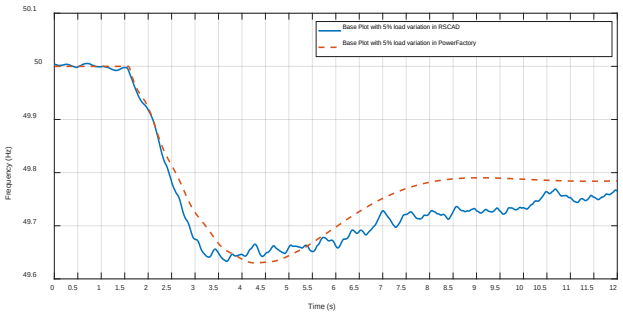

Figure 8. Frequency response due to load increase at bus 8 in RMS (PowerFactory) and EMT (RSCAD) simulations.

A. *Impact of droop-based FAPI controller:*

The droop based FAPI controllers should be activated when the frequency deviation is in the range of 0.06% to 0.1% of the nominal frequency value.

Figure 9 depicts the frequency plots obtained for a system with and without a FAPI controller. According to the obtained results, considerable improvement in Nadir can be achieved after activation of droop based FAPI controller. This improvement is due to the fast active power injection, as the output of FAPI controller of wind generation unit, to compensate the frequency drop after the fault. Figure 10 represents the power injected by the wind turbine with activated droop based FAPI controller with K_p set to 0.7. According to these results, the variation of power output is less than 10% on the nominal power of the wind turbine [22] and [26].

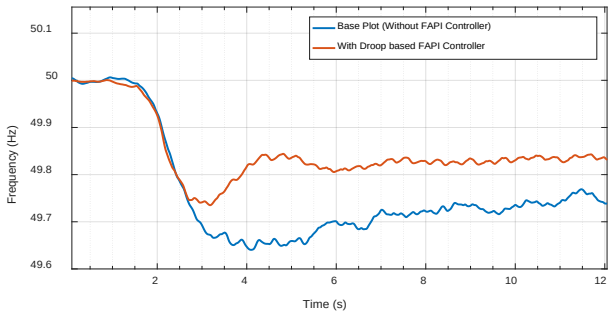

Figure 9. Frequency response with droop based FAPI controller at wind genertors, due to a load increase at bus 8.

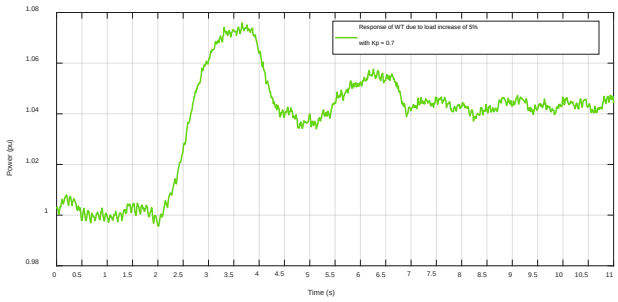

Figure 10. The response of wind turbine for 5% load variation with 52% wind share with activated proportional based FAPI controller in RSCAD.

Figure 11 depicts the frequency plots obtained for various proportional gains in reference to droop controller. As noticed from the figure, when K_p=0 is the base plot where a droop controller is deactivated. As the value of K_p is increased, the influence of droop based FAPI controller in frequency regulation increases, and as a result, Nadir improvement is witnessed. This can be corroborated in the plots of K_p = 0.4, 0.5, 0.7. But the further increase in K_p is leading to oscillations in frequency making the system behave as an under-damped system, causing a varying generation dispatch from wind generators. This is evident from the plots of K_p = 1 and 1.5.

Hence for K_p = 0.7, the best results were observed with a Nadir shift from 49.64 Hz (base case) to 49.78Hz, which is an improvement of 38.88%.

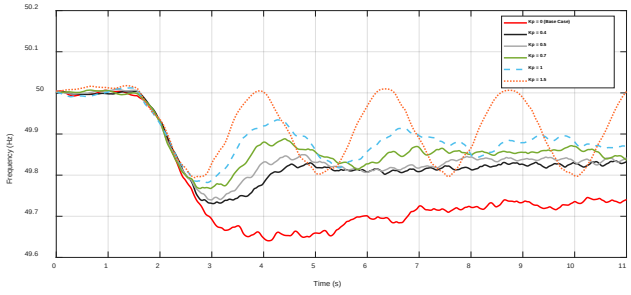

Figure 11. Frequency response due to load increase at bus 8 with proportional based FAPI controller at WG's.

B. Impact of derivative-based FAPI controller:

This section presents the results obtained for the derivative-based FAPI controller which was described in Section II. It is expected that the addition of derivative control loop can have improvement on the slope of the frequency during the containment period. In order to give more insight into the impact of the proposed controller, a complete sensitivity analysis is perfomed with different values of the FAPI controller gains.

Figure 12 depicts the frequency plots obtained for various values of proportional (K_p) and derivative gains (K_d) in reference to the derivative-based FAPI controller. The values selected here are the possible combinations of K_p and K_d achieved by tuning.

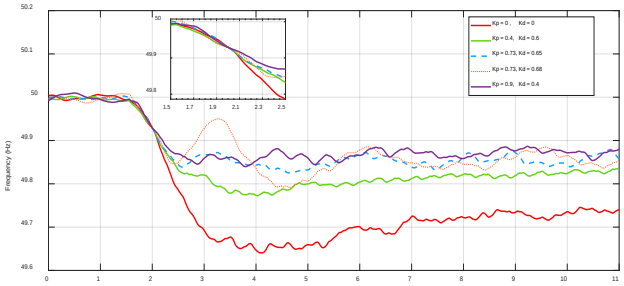

Figure 12. Frequency response due to load increase at bus 8 with derivative-based FAPI controller at WG's.

As shown in Figure 12 the red curve, the plot with K_p = 0 and K_d = 0, forms the base plot without FAPI controller. With K_p = 0.4 and K_d = 0.6, it can be observed that since K_p value is less, nadir improvement is a comparatively lower but considerable improvement in dynamic frequency response before nadir can be observed. While the plot with K_p=0.9 and K_d=0.4 gave the best performance considerable improvements I both RoCoF and Nadir. (with RoCoF improvement from 280 mHz/sec (base case) to 139.7 mHz/sec and Nadir shift from 49.64 Hz (base case) to 48.845 Hz). It should be noted that the RoCoF is calculated for a time window of 500 ms after the occurrence of the fault.

Figure 13 shows the comparison between the different FAPI controllers (Droop based and Derivative based controllers) that can be implemented in a Type-4 wind generator. The best plot from each of the controller is taken to compare. From the obtained results, it can be noticed that the best performance is from the derivative-based FAPI controller which improves both Nadir and RoCoF.

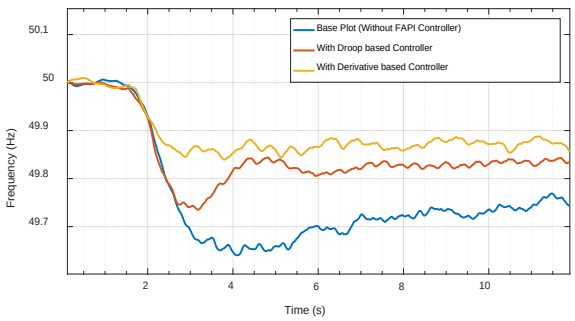

Figure 13. Frequency response due to load increase at bus 8. Comparisons with different FAPI controllers).

IV. Conclusions

Two different fast active power injection (FAPI) controllers were implemented on a wind generator Type-4 in both RMS and RSCAD platforms. The first method was the droop based FAPI (the most common approach) and the second method was the modified derivative-based FAPI controller which consists of combining methods for droop control and frequency derivative-based control.

A detailed sensitivity analysis for the control parameters was presented to show the impact of the controller on wind turbine active power injection for mitigation of frequency stability issue. Based on RMS simulations and EMT simulations, it was found that the modified derivative-based FAPI constitutes effective solutions for mitigation of frequency Nadir and RoCoF (computed in the time window of 0.5s from the time of occurrence of an active power imbalance).

For the studied test power systems, it was observed that these methods could help to increase the share of wind power generation in future power systems. The boundaries for effectiveness and flexibility of these methods are defined by the source of energy used to support fast active power injection and the technical limit of the power electronic converter used to interconnect with the power system. Current technologies and inner control methods of power electronic converters allow around 10% overload during 10s. In both FAPIs, the controller gains were chosen so as to increase active power injection in steps by around 10% over the rated value during the containment period.

Acknowledgment

This research was carried out as part of the MIGRATE project. This project has received funding from the European Union's Horizon 2020 research and innovation program under grant agreement No 691800. This reflects only the authors' views and the European Commission is not responsible for any use that may be made of the information it contains.

References

[1] P. Kundur et al., "Definition and Classification of Power System Stability," IEEE Trans. Power Syst., vol. 19, no. 3, pp. 1387–1401, 2004.

[2] P. Tielens and D. Van Hertem, "The relevance of inertia in power systems," Renew. Sustain. Energy Rev., vol. 55, pp. 999–1009, 2016.

[3] E. Rakhshani, J. Sadeh, "Practical Viewpoints on Load Frequency Control Problem in a Deregulated Power System", Energy conversion and management, Vol. 51. Issue 6. pp. 1148-1156. June 2010.

[4] E. Rakhshani, D. Gusain, V. Sewdien, Jose Luis Rueda Torres, Mart Van der Meijden, "A Key Performance Indicator to Assess the Frequency Stability of Converter Dominated Power System", IEEE Access, ACCEPTED, 2019.

[5] H Mehrjerdi, "Simultaneous Load Leveling and Voltage Profile Improvement in Distribution Networks by Optimal Battery Storage Planning", Energy, vol 181, pp. 916-926, 2019.

[6] E. Rakhshani, D. Remon, P. R. Cortes, "Modeling and Sensitivity Analyses of VSP based Virtual Inertia Controller in HVDC links of Interconnected Power Systems", Electric Power systems Research, Elsevier, vol. 141, pp. 246–263, 2016.

[7] Hasan Mehrjerdi, Elyas Rakhshani, "Optimal operation of hybrid electrical and thermal energy storage systems under uncertain loading condition," Applied Thermal Engineering, Elsevier, Vol. 160, 2019.

[8] E. Rakhshani, J. Luis Rueda Torres, M. van der Meijden, and Peter Palensky, "Determination of Maximum Wind Power Penetration Considering Wind Turbine Fast Frequency Response", POWERTECH 2019, Italy, 2019.

[9] Hasan Mehrjerdi, Elyas Rakhshani, "Vehicle-to-grid technology for cost reduction and uncertainty management integrated with solar power," Journal of Cleaner Production, Elsevier, Vol .229, pp. 463-469, 2019.

[10] E. Rakhshani, P. R. Cortes, "Inertia Emulation in AC/DC Power Systems Using Derivative Technique Considering Frequency Measurement Effects", IEEE Transactions on Power Systems, Volume: 32, Issue: 5, 2017.

[11] R. Eriksson, N. Modig, and K. Elkington, "Synthetic inertia versus fast frequency response : a definition," IET Renew. Power Gener., vol. 12, no. 5, pp. 507–514, 2018.

[12] M. Dreidy, H. Mokhlis, and S. Mekhilef, "Inertia response and frequency control techniques for renewable energy sources : A review," Renew. Sustain. Energy Rev., vol. 69, no. July 2016, pp. 144–155, 2017.

[13] F. Ha and A. Abdennour, "Optimal use of kinetic energy for the inertial support from variable speed wind turbines," Renew. Energy, vol. 80, pp. 629–643, 2015.

[14] E. Rakhshani, D. Remon, A. M. Cantarellas, and P. R. Cortes, "Analysis of Derivative Control-Based Virtual Inertia in Multi-Area HVDC Interconnected AGC Power Systems," IET Generation Transmission & Distribution, vol. 10, no. 6, pp. 1458-1469, 2016.

[15] M. Dreidy, H. Mokhlis, S. Mekhilef, "Inertia response and frequency control techniques for renewable energy sources: A review," Renewable and Sustainable Energy Reviews, vol. 69, pp. 144–155, 2017.

[16] Gonzalez-Longatt F.M., "Effects of the synthetic inertia from wind power on the total system inertia: simulation study," IEEE environment friendly energies and appl conference; pp. 389–95, 2012.

[17] H. Knudsen, JN. Nielsen, Introduction to the modelling of wind turbines: Wind Power in Power Systems, Second Edition, 2005.

[18] F. Gonzalez-Longatt, E. Chikuni, E. Rashayi, "Effects of the synthetic inertia from wind power on the total system inertia after a frequency disturbance," Proceedings of IEEE Ind Technol Conference, 2013.

[19] S. Mishra, P. Zarina, P. Sekhar, "A novel controller for frequency regulation in a hybrid system with high PV penetration," In: IEEE Power and Energy Soc General Meeting (PES), p. 1–5, 2013.

[20] R. Josephine, S. Suja, "Estimating PMSG wind turbines by inertia and droop control schemes with intelligent fuzzy controller in Indian," Dev J Elect Eng Technol, vol. 9, pp. 1196–201, 2014.

[21] W. Yao, K.Y. Lee, "A control configuration of wind farm for load-following and frequency support by considering the inertia issue," Proceedings of IEEE Power and Energy Soc General Meeting, 2011.

[22] S. Engelken, A. Mendonca and M. Fischer, "Inertial response with improved variable recovery behaviour provided by type 4 WTs," IET Renewable Power Generation, vol. 11, no. 3, pp. 195-201, 2017.

[23] RSCAD - POWER SYSTEM SIMULATION SOFTWARE – RTDS, [Online]. Available: https://www.rtds.com/the-simulator/our-software/about-rscad/. [Accessed: 18-Jun.-2019].

[24] SIMULATION MODELLING LIBRARIES, RTDS Technologies Inc., [Online]. Available: https://www.rtds.com/the-simulator/our-software/modelling-libraries/. [Accessed: 18-Jun.-2019].

[25] J. Fang, H. Li, Y. Tang, and F. Blaabjerg, "On the Inertia of Future More-Electronics Power Systems," IEEE J. Emerg. Sel. Top. Power Electron., 2018.

[26] J. Morren, W.H. de haan, Wil L. kling, J. A. Ferreira, "Wind Turbine Emulating Inertia and Supporting Primary Frequency Control," IEEE Transactions on Power Systems, vol. 21, No. 1, 2006.